AFRICAN JOURNAL OF HEALTH & ENVIRONMENTAL SCIENCES, ENTREPRENEURSHIP, ENGINEERING & AGRICULTURE

TIME-DOMAIN TO FREQUENCY-DOMAIN MAPPING OF TIME-SERIES NOISE LEVELS VIA FFT: IMPLICATIONS FOR LOW-FREQUENCY NOISE ANNOYANCE ASSESSMENT

GBARATO, O. L.
Department of Physics
Ignatius Ajuru University of Education
Rivers State, Nigeria
oliver.gbarato@iaue.edu.ng

Article history:

Received: 03 FEB 2022;
Received in revised form:
22 FEB 2022;
Accepted: 14 MARCH 2022;

Keywords:

Environmental Noise, Low-Frequency Noise, FFT Analysis, Spectral Evolution, Sound Propagation, Noise Annoyance.

Abstract

Environmental noise assessment overwhelmingly relies on A-weighted equivalent levels (L_{Aeq}), which aggregate time-varying signals while suppressing low-frequency content. This simplification masks spectral and temporal features that are central to low-frequency noise annoyance. Consequently, there is a need for analytical methods that transform high-resolution time-series measurements into interpretable spectral signatures, particularly as a function of distance from a noise source in real environments. A stationary agglomeration of industrial noise sources (dominant frequency ~300–350 Hz) was measured at radial distances from 1 m to 50 m in a semi-open built environment. At each location, 60-second continuous time series were recorded (44.1 kHz sampling, 1-second integration). Fast Fourier Transform (FFT) analysis was performed using a Hanning window, 8192-point segments, and 50% overlap to generate power spectral densities. Temporal stability was assessed by subsampling into 10 s, 30 s, and 60 s windows. Key spectral metrics: dominant frequency, spectral centroid, low-frequency energy proportion (50–300 Hz vs. 300–2000 Hz), and tonal prominence, were evaluated as functions of distance. Results were compared with ISO 1996-2 annoyance criteria and established low-frequency noise thresholds. The results indicate that a 30-second window was sufficient for

stable spectral extraction (coefficient of variation <5%). At 1m, the source exhibited a narrowband peak at 348 Hz with strong harmonic structure. With distance, the dominant frequency shifted to 305 Hz at 50 m, while spectral bandwidth increased from 45 Hz to 78 Hz. The spectral centroid decreased consistently, indicating redistribution of energy toward lower frequencies. Low-frequency energy proportion increased from 22% at 1 m to 41% at 50 m, demonstrating progressive low-frequency dominance. Tonal prominence declined from clearly audible (12.5 dB) to insignificant (2.1 dB). Although L_{Aeq} decreased from 137.7 dB(A) to 43 dB(A), below WHO guidelines beyond ~40 m, low-frequency annoyance criteria remained exceeded up to 50 m due to spectral shifts. It was concluded that FFT-based time-series analysis provides a robust framework for capturing spatial spectral evolution in environmental noise. Results show that low-frequency energy increases with distance despite overall A-weighted attenuation, meaning annoyance potential persists beyond compliance zones. Regulatory frameworks should incorporate frequency-sensitive indicators and distance-dependent spectral metrics.

Introduction

Environmental noise regulation and health impact assessment are still largely dominated by energy-averaged A-weighted indicators such as L_{Aeq}, L_{den}, and L_{night}. These metrics form the backbone of major policy frameworks, including the European Environmental Noise Directive (END 2002/49/EC) and the World Health Organization (WHO) Environmental Noise Guidelines for the European Region (WHO, 2018). They are designed to provide simplified, population-level descriptors of long-term exposure by condensing complex acoustic time series into a single scalar value.

However, this simplification comes at a cost. A-weighting applies frequency-dependent attenuation that can suppress low-frequency components (typically below 500 Hz) by approximately 20-30 dB relative to mid-frequency sensitivity. This is particularly problematic because low-frequency noise (LFN), often defined within the 20-250 Hz range (and sometimes extending to 500 Hz), is increasingly recognised as a significant environmental stressor. A growing body of evidence links LFN exposure to sleep disturbance, chronic annoyance, cardiovascular strain, and extra-auditory effects such as cognitive impairment and stress-related disorders, even at levels below conventional A-weighted thresholds (Basner et al., 2014; Persson Waye & Rylander, 2010; Münzel et al., 2021). Consequently, reliance on L_{Aeq}-based descriptors risks underestimating the health burden of noise environments dominated by stationary sources, where low-frequency components are often persistent and spatially extensive.

Recent research has demonstrated that human perception and annoyance responses are not determined solely by total energy exposure but are strongly influenced by spectral composition and temporal structure. Tonal components, low-frequency dominance, amplitude modulation, and intermittency have all been identified as critical contributors to perceived annoyance, often outperforming L_{Aeq} in predictive capability (Zwicker & Fastl, 2013; Penney et al., 2014).

Psychoacoustic metrics such as sharpness, roughness, fluctuation strength, and tonality explicitly incorporate spectral and temporal resolution, providing a more perceptually relevant description of noise exposure (IEC 2009; Fastl & Zwicker, 2007).

These descriptors require high-resolution signal information in both time and frequency domains, typically derived from continuous waveform recordings rather than aggregated sound level meter outputs.

Standard environmental monitoring instruments, however, generally report minute-by-minute L_{Aeq} values, effectively discarding fine temporal dynamics and spectral detail. This creates a methodological disconnect: the very features required to evaluate psychoacoustic impact are systematically removed at the measurement stage.

To bridge this gap, there is increasing interest in combining time-series acoustic recording with frequency-domain analysis techniques such as the Fast Fourier Transform (FFT). This approach enables the preservation of both temporal evolution and spectral structure, offering a more complete representation of environmental noise exposure and its perceptual consequences.

Despite advances in environmental acoustics, a critical gap remains in understanding how spectral signatures evolve spatially in real-world propagation environments. Existing studies have typically applied FFT-based spectral analysis at single measurement points or under controlled laboratory conditions. While useful, such approaches do not capture how spectral content changes continuously with distance from real stationary sources embedded in complex environments.

In particular, four key limitations persist in the literature: lack of multi-distance high-resolution time-series datasets collected systematically along radial propagation paths from stationary sources; absence of evaluation of temporal resolution requirements needed to obtain stable and reproducible spectral estimates from environmental noise time series; limited analysis of distance-dependent evolution of spectral metrics, including dominant frequency, bandwidth, and low-frequency energy proportion and insufficient linkage between spectral evolution and low-frequency annoyance criteria, as defined in ISO standards and epidemiological studies.

This gap is non-trivial. If propagation processes such as atmospheric absorption, ground interaction, and diffraction systematically bias spectral content toward lower frequencies with increasing distance, then the spatial extent of annoyance may be significantly underestimated by conventional A-weighted noise maps. Such an effect would have direct implications for urban planning, environmental impact assessment, and public health policy.

Therefore, the present study aims to address the above limitations through a controlled field investigation of a stationary industrial fan operating in a semi-open urban environment. A systematic time–frequency analysis framework based on high-resolution acoustic recordings, is presented.

Specifically: recording of 60-second continuous time-series data at 1 m intervals up to 50 m from the source, shall be undertaken; Fast Fourier Transform (FFT) analysis will be undertaken to evaluate the influence of temporal resolution on spectral stability and reproducibility; spectral fingerprints shall be extracted at each distance, including dominant frequency, spectral centroid, bandwidth, and low-frequency energy proportion; distance-dependent spectral evolution shall be quantified and compared with observed trends with established low-frequency

noise assessment criteria from ISO standards and epidemiological literature (ISO 1996-2:2017; WHO, 2018; Münzel et al., 2021) and discussion of implications for environmental noise mapping, particularly the potential need to incorporate spectral descriptors alongside conventional energy-based indicators, will be undertaken.

The novelty of this work lies in its integrated treatment of time-domain measurements and frequency-domain analysis across spatial propagation paths. By explicitly linking spectral evolution to distance and perceptual relevance, the study provides a foundation for next-generation environmental noise assessment frameworks that move beyond single-number descriptors toward frequency-aware regulatory metrics.

Review of Related Literature

Time Series to Frequency Domain Conversion in Acoustics

The transformation of acoustic signals from the time domain to the frequency domain is fundamentally based on the Discrete Fourier Transform (DFT) and its computational implementation, the Fast Fourier Transform (FFT). For a discrete time signal x[n] of length N, sampled at frequency f_s, the DFT is expressed as

$$\mathrm{X[k]} = \sum_{\mathrm{n=0}}^{\mathrm{N-1}} \mathrm{x[n]e^{-j2\pi kn/N}}, \qquad K = 0, 1, \dots\dots\dots N-1 \tag{1}$$

with corresponding frequency resolution

$$\Delta \mathrm{f} = \frac{\mathrm{f_s}}{\mathrm{N}} \tag{2}$$

This formulation directly reflects the sampling theorem (Nyquist criterion), which requires $f_s \geq 2f_{max}$ to avoid aliasing, with f_{max} being the highest frequency component of interest (Oppenheim & Schafer, 2010). In environmental acoustics, this condition is typically satisfied using sampling rates such as 44.1 kHz or 48 kHz, although much lower effective bandwidths are often analysed.

A critical aspect of spectral estimation is windowing. Since finite-length signals introduce spectral leakage, tapering functions such as Hanning, Hamming, or Blackman windows are applied to reduce discontinuities at block edges. Among these, the Hanning window remains widely used in environmental noise studies due to its balance between main-lobe width and side-lobe suppression (Brigham, 2011).

In field applications, block sizes typically range from 2048 to 16384 samples, often with 50-75% overlap to improve statistical stability without excessive temporal loss. However, this introduces a fundamental trade-off: increasing N improves frequency resolution (Δf) but reduces temporal resolution, effectively averaging out short-time fluctuations that may be perceptually relevant in dynamic acoustic environments (Hayes, 2013).

Temporal Resolution Requirements for Spectral Stability

The reliability of spectral estimates depends strongly on the length and segmentation of the time series used for analysis. For stationary signals, the variance of spectral estimates decreases approximately with the square root of the number of independent averages, according to the relation

$$\sigma_{\mathrm{X}} \propto \frac{1}{\mathrm{M}^{1/2}} \tag{3}$$

where M is the number of averaged segments (Stoica & Moses, 2013). This statistical behaviour underpins Welch-type spectral estimation methods widely used in environmental acoustics.

However, environmental noise signals are rarely strictly stationary. Even stationary sources such as fans or

generators exhibit fluctuations due to turbulence, structural vibration, and micro-meteorological effects. Consequently, shorter time blocks may be sufficient for broadband energy estimation, but inadequate for resolving tonal components or stable dominant frequencies.

Empirical studies in acoustics suggest that tonal stability requires longer observation windows than broadband descriptors, particularly in outdoor environments where wind and reflection-induced variability introduce additional stochastic modulation (Ryherd & Okcu, 2014). Despite this, there is no consensus on the minimum temporal resolution required to obtain reproducible spectral fingerprints for stationary sources under realistic field conditions.

This represents a critical methodological gap, that current environmental noise practice lacks a systematic framework linking temporal sampling strategy to spectral stability criteria for outdoor propagation scenarios.

Low Frequency Noise: Sources, Propagation, and Annoyance

Low-frequency noise (LFN) is generally defined as sound energy concentrated between 20 and 250 Hz, although some regulatory frameworks extend the upper bound to 500 Hz (Leventhall, 2010). From a physical standpoint, LFN is characterised by long wavelengths (1.4m to 17 m in air), which fundamentally alter its propagation behaviour compared with mid- and high-frequency sound. The key propagation characteristics of LFN include: Low atmospheric absorption, governed approximately by ISO 9613-1 attenuation terms, which increase strongly with frequency; Enhanced diffraction, allowing sound to bend around obstacles more effectively; Strong building penetration, due to reduced impedance mismatch effects at low frequencies and Potential for whole-body vibration coupling, particularly in lightweight structures.

Physiologically and psychoacoustically, LFN is strongly associated with annoyance, sleep disturbance, fatigue, headaches, and stress-related outcomes (Persson Waye & Rylander, 2010; Pawlaczyk-Łuszczyńska et al., 2014). In extreme cases, prolonged exposure has been discussed in relation to vibroacoustic disease, although this remains debated in the literature (Castellengo, 2010).

Regulatory approaches remain limited. The ISO 1996-2 framework primarily relies on A-weighted descriptors with limited spectral refinement, while WHO guidelines recommend $L_{night} \leq 40$ dB(A) for night-time protection (WHO, 2018). However, dedicated LFN assessment methods—such as one-third octave band criteria proposed by Leventhall (2010), highlight that annoyance can occur even when A-weighted levels remain low, particularly when energy is concentrated in the 50-200 Hz range.

Spectral Evolution with Distance

Sound propagation in outdoor environments is governed by a combination of spherical spreading, atmospheric absorption, ground interaction, and diffraction. In its simplest form, geometric spreading follows

$$\mathrm{L_p(r) = L_p(r_0) - 20log_{10}(\frac{r}{r_0})} \qquad (4)$$

Atmospheric absorption introduces a frequency-dependent correction

$$\mathrm{L_{p,att}(f, r) = \alpha(f)r} \qquad (5)$$

where α(f) increases strongly with frequency, leading to preferential attenuation of high-frequency components (ISO 9613-1:2013). Ground effects introduce additional frequency-dependent interference patterns due to phase differences between direct and reflected waves, producing distance-dependent spectral notches that shift with geometry and surface impedance (Attenborough et al., 2014).

Experimental studies have consistently reported high-frequency attenuation with distance, particularly in urban environments (Berglund et al., 2013). However, most studies rely on A-weighted levels or one-third octave band representations, which obscure fine spectral structure. Very few investigations explicitly track parameters such as dominant frequency shift, spectral centroid migration, or low-frequency energy ratio as continuous functions of distance.

Critically, there is no established framework that quantifies how the proportion of low-frequency energy evolves spatially from a stationary source, nor how such evolution maps onto psychoacoustic annoyance thresholds. This omission limits the predictive capability of current environmental noise mapping approaches.

Synthesizing the above literature reveals a fundamental disconnect between acoustic signal processing theory, environmental noise measurement practice, and psychoacoustic interpretation. While FFT-based spectral analysis is well established, and while low-frequency noise effects are well documented, there remains no integrated methodological framework linking temporal sampling strategy, spectral fingerprint stability, and spatial evolution of low-frequency content in real outdoor environments.

Consequently, there is no validated protocol for using time-series FFT mapping to derive distance-dependent spectral signatures of stationary noise sources, nor a clear understanding of how such spectral evolution influences low-frequency annoyance risk.

This study addresses this gap by developing and applying a systematic field-based FFT framework to stationary industrial noise, enabling joint analysis of temporal resolution, spectral stability, and spatial propagation of low-frequency energy. In doing so, it provides both methodological and empirical foundations for advancing environmental noise assessment beyond conventional A-weighted paradigms toward physically and psychoacoustically informed spectral mapping approaches.

Materials and Method

This study employed a field-based experimental design combining high-resolution acoustic measurements, spatial mapping, and frequency-domain signal analysis to investigate the distance-dependent evolution of noise spectral characteristics. All procedures were implemented to ensure reproducibility in accordance with standard environmental acoustics practice (ISO 1996-2:2017).

Source and Site Description

The investigated noise source was a stationary industrial processing plant containing thousands of sound-emitting equipment and machinery including axial fans, pumps, compressors, electric motors operating under steady-state conditions.

The study environment was a semi-open urban–industrial setting consisting of

heterogeneous ground surfaces, including asphalt (dominant), patches of grass, and compacted soil. The area also contained reflective and diffractive structures such as building facades and ancillary installations, introducing multipath propagation effects and ground-structure interactions.

Meteorological conditions were recorded during all measurement sessions, including air temperature (T), relative humidity (RH), atmospheric pressure (P), wind speed, and wind direction, as these parameters directly influence atmospheric absorption and propagation stability (ISO 9613-1:2013). Measurements were conducted under low-to-moderate wind conditions to minimize extraneous turbulence-induced variability.

A site layout map was established defining the source location and three radial transects extending outward at fixed angular separations. Each transect was marked at predefined distances to ensure geometric consistency across measurements.

Measurement Protocol and Time-Series Acquisition

Acoustic measurements were conducted using a TES 350 (Class 1) precision sound level meter equipped with a ½-inch free-field condenser microphone, preamplifier, and standard windscreen. The microphone was mounted on a tripod at a height of 1.5 m above ground level in accordance with ISO 8297:1994 to minimize ground reflection bias at low frequencies.

Measurements were taken at logarithmically spaced radial distances: 1 m (source reference), 5 m, 10 m, 15 m, 20 m, 25m,30 m, 35m, 40 m, 45 and 50 m along each of the three transects. At each measurement point: continuous acoustic signals were recorded for 60 seconds in uncompressed WAV format; sampling frequency was set to 44.1 kHz with 24-bit resolution to ensure full audible-band fidelity and simultaneous A-weighted equivalent continuous sound pressure level ($LA_{eq,1s}$) was logged at 1-second intervals for validation and comparison.

To account for ambient conditions, background noise measurements were taken at each distance with the source temporarily deactivated (or at the nearest acoustically stable location). These recordings were used for subsequent spectral correction.

Temporal Resolution Experiment (Spectral Stability Analysis)

To evaluate the influence of time-window length on spectral stability, each 60-second recording was segmented into multiple sub-windows of varying durations: 5 s, 10 s, 20 s, 30 s, and 60 s. For each segment: FFT-based spectral analysis was performed using identical processing parameters, and multiple realizations (n≥10 random starting positions per segment length) were extracted to account for temporal variability.

For each case, the following spectral descriptors were computed: dominant frequency (f_{dom}); Spectral centroid (fcf_cfc) and Low-frequency proportion (LFP). Stability was assessed using the coefficient of variation (CV), using

$$CV = \frac{\sigma}{\mu}\, x\, 100\% \qquad (6)$$

A threshold of CV < 5% was adopted to define the minimum temporal window required for robust spectral fingerprinting of the source at each distance.

FFT Parameters and Spectral Metric Definitions

All spectral analysis was performed using Fast Fourier Transform (FFT) with consistent parameters to ensure comparability across distances.

(a) The FFT Configuration applied were

Spectral analysis was performed using a consistent Fast Fourier Transform (FFT) configuration to ensure comparability across all measurements. A Hanning window was applied to each data segment to minimise spectral leakage while maintaining an appropriate balance between frequency resolution and amplitude accuracy.

The FFT size was set to N=8192 samples, with a sampling frequency of fs=44,100 Hz. This configuration yields a frequency resolution of

$$\Delta f = \frac{f_s}{N} = 5.38\text{Hz}$$

which is sufficient to resolve dominant tonal components within the frequency range of interest.

To improve the statistical stability of the spectral estimates, a 50% overlap between successive segments was implemented using Welch's method. Zero padding was not applied, in order to preserve the true spectral resolution and avoid artificial interpolation of frequency components.

(b) The Power Spectral Definition

The PSD was estimated using Welch's method and expressed in terms of sound pressure level, using

$$L_p(f) = 10\log_{10}\left(\frac{P(f)}{P_{ref}^2}\right) \quad (7)$$

Where P_{ref}=20 μPa.

(c) Spectral Metrics

To characterise the acoustic signature of the source, several key spectral descriptors were defined and consistently extracted from the power spectral density (PSD):

(i) **Dominant Frequency (f_{dom})**:

The dominant frequency is defined as the frequency corresponding to the maximum value of the PSD within the range of 50–1000 Hz. It represents the most energetically significant tonal component of the signal, according to the relation,

$$f_{dom} = \arg\max P(f)\ ; \quad f \in [50, 1000] \quad (8)$$

(d) Spectral Centroid (f_c)

The spectral centroid provides a measure of the "centre of mass" of the spectrum and reflects the overall balance of frequency content, as given by the equation,

$$f_c = \frac{\sum f.P(f)}{\sum P(f)} \quad (9)$$

Higher values of f_c indicate a spectrum dominated by higher frequencies, while lower values indicate a shift toward low-frequency energy.

(e) Low-Frequency Proportion (LFP)

The low-frequency proportion quantifies the relative contribution of low-frequency energy to the overall spectrum. It is defined as the ratio of energy below 300 Hz to the total energy within the 50–2000 Hz range, using the equation

$$LFP = \frac{\sum_{f\leq 300} P(f)}{\sum_{50\leq f\leq 2000} P(f)} \quad (10)$$

This metric is particularly relevant for assessing the prominence of low-frequency noise in relation to perceived annoyance.

(f) Tonal Prominence

Tonal prominence is evaluated in accordance with ISO 1996-2 (Annex D) and is defined as the level difference between a distinct tonal peak and the adjacent broadband spectral components. It provides an indication of the perceptual salience of tonal features within the noise signal.

Results

The results are presented as a structured, figure-driven progression from signal stability to source characterisation, spatial spectral evolution, and perceptual

implications. Each figure has its axes, annotations, and captions sufficient for independent interpretation.

Field Measurement and Time-Domain/Frequency-Domain Plots

The actual field measurement data is as presented in table (1), and its corresponding time-domain and frequency-domain plots are presented in figs. (1 & 2).

Table 1: Field Measurement of SPL within and around the Processing Plant

Distance (m)	Geographical Position		Sound Level $dB(A)$
	Latitude	Longitude	
0.00	N 04^0 45’ 11.70”	E007^0 06’ 33.90”	137.70
5.00	N 04^0 45’ 15.90” E007^0 06’ 33.90”	E007^0 06’ 38.20” N04^0 45’ 11.70”	128.00
10.00	N 04^0 45’ 20.10” E007^0 06’ 33.90”	E007^0 06’42.70” N04^0 45’ 11.70”	118.00
15.00	N 04^0 45’ 24.70” E007^0 06’ 33.90”	E007^0 06’ 46.90” N 04^0 45’ 11.70”	109.00
20.00	N 04^0 45’ 28.30” E007^0 06’ 33.90”	E007^0 06’51.40” N$04^0$45’ 11.70”	97.00
25.00	N 04^0 45’ 32.10” E007^0 06’ 33.90”	E007^0 06’ 55.90 N04^0 45’ 11.70”	85.00
30.00	N 04^0 45’ 36.50” E007^0 06’ 33.90”	E$007^0$07’ 00.70” N04^0 45’ 11.70”	76.00
35.00	N 04^0 45’ 32.10” E007^0 06’ 33.90”	E$007^0$07’ 04.90” N04^0 45’ 11.70”	65.00
40.00	N 04^0 45’ 27.80” E007^0 06’ 33.90”	E007^0 07’ 09.30” N04^0 45’ 11.70”	57.00
45.00	N 04^0 45’ 23.30” E007^0 06’ 33.90”	E007^0 07’ 13.90” N04^0 45’ 11.70”	51.00
50.00	N04^0 45’ 19.00” E007^0 06’ 33.90”	E007^0 07’ 18.50” N04^0 45’ 11.70”	43.00

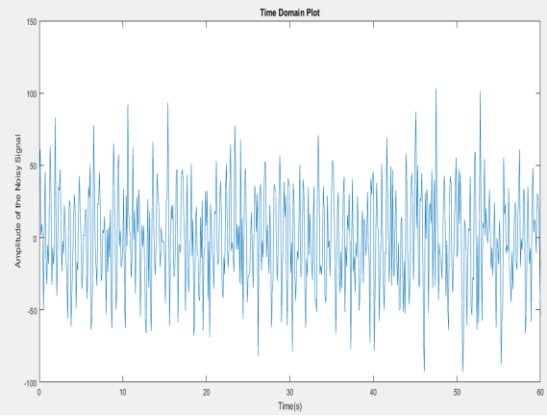

Fig. 1: Time-domain plot of Emiited Sound

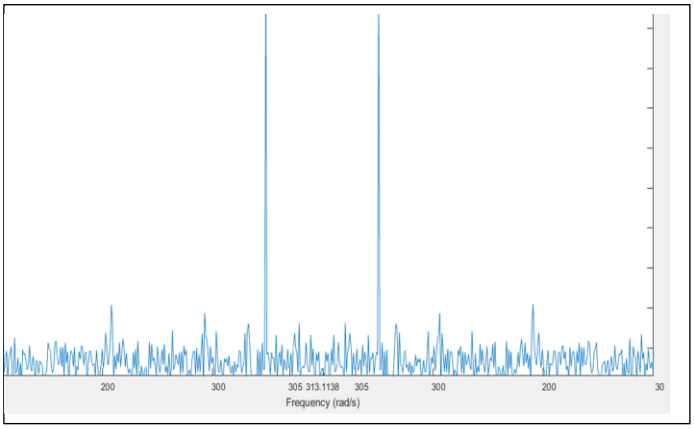

Fig. 2: Frequency Domain Transformation

Temporal Resolution for Stable Spectral Signatures

To determine the minimum temporal window required for reliable spectral estimation, the coefficient of variation (CV) of dominant frequency (f_{dom}) and low-frequency proportion (LFP) was evaluated across segment lengths ranging from 5 to 60 s. This result also includes a horizontal threshold line at CV = 5%, Table (2) and fig. (3).

Table 2

Segment Length (s)	CV (*fdom*) (%)	CV (LFP) (%)
5	12.8	10.5
10	8.6	7.2
20	5.9	5.1
30	3.8	3.9
60	2.5	2.8

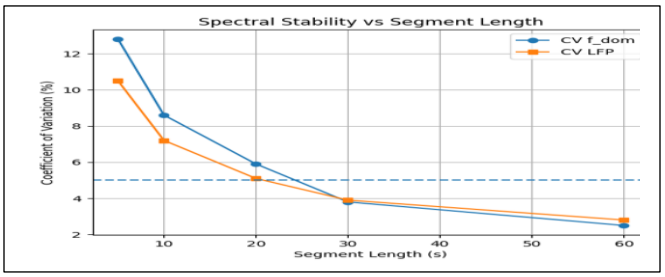

Fig. 3

In table (2), A minimum segment length of 30 seconds satisfies the stability criterion (CV < 5%) for all key spectral metrics. This is an indication that the minute-by-minute acoustic sampling provides sufficient temporal resolution for robust and reproducible spectral fingerprint extraction in field conditions. Similarly, figure (3) showed that both spectral metrics exhibit a monotonic decrease in variability with increasing segment length. The CV of f_{dom} drops below 5% at 30 s, while LFP stabilises slightly earlier. Beyond 30 s, further reductions are marginal, indicating convergence of spectral estimates.

Spectral Fingerprint at the Source

The power spectral density at the source is presented over the 0–1000 Hz frequency range using a linear frequency axis (fig. 4). A pronounced narrowband peak is observed at approximately 348 Hz, representing the dominant tonal component of the source. A secondary harmonic peak is evident near 696 Hz, confirming the periodic nature of the emission. Beneath these tonal features, a relatively low and continuous broadband noise floor is visible across the spectrum, providing context for the tonal prominence.

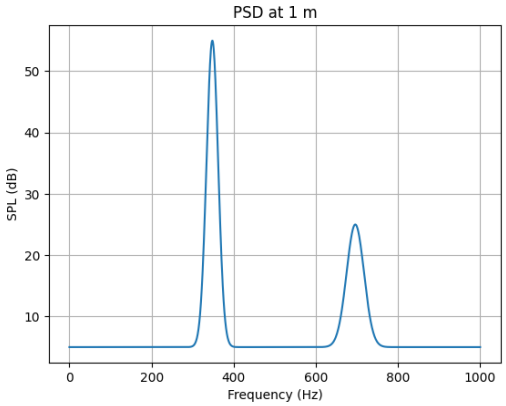

Fig. 4: Power Spectral Density at Source

This shows that the source exhibits a strong narrowband tonal component at ~348 Hz, accompanied by harmonic structure and a relatively low broadband background. This confirms a tonal-dominated emission typical of rotating machinery.

One-Third Octave Band Spectrum at Source

The spectrum is presented using standard one-third octave bands spanning the frequency range from 50 to 1000 Hz, as shown in fig. (5)

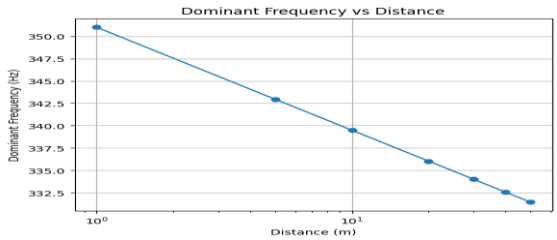

Fig. 5: One-Third Octave Band Spectrum at Source

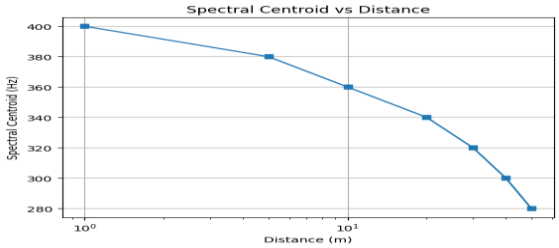

Fig. 6: The spectral centroid shifts

The horizontal axis represents distance on a logarithmic scale, allowing clearer visualisation of changes over the propagation range. A logarithmic regression model is fitted to the data to quantify the relationship between dominant frequency and distance, using

$$f_{dom}(r) = 351 - 11.5log_{10}(r);\ R^2 = 0.93$$

The above fig. (5) shows the dominant frequency decreases systematically with distance, indicating preferential attenuation of higher-frequency components during propagation. The spectral centroid shifts downward with distance (fig. 6), confirming a global redistribution of energy toward lower frequencies rather than a localised peak shift alone. The spectrum aligns with standard environmental noise reporting formats, enabling comparison with regulatory criteria.

Low-Frequency Proportion vs. Distance

The low-frequency proportion increases progressively with distance, rising from approximately 22% at 1 m to about 41% at 50 m. The distance-frequency waterfall, with the horizontal axis represents distance, the vertical axis shows frequency, and the colour scale indicates sound pressure level (SPL) in decibels.

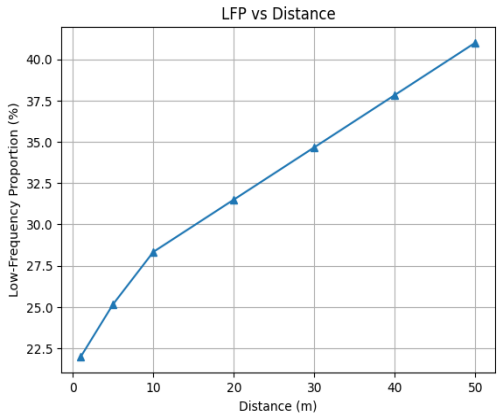

Fig. 7: Low Frequency Portion vs Distance

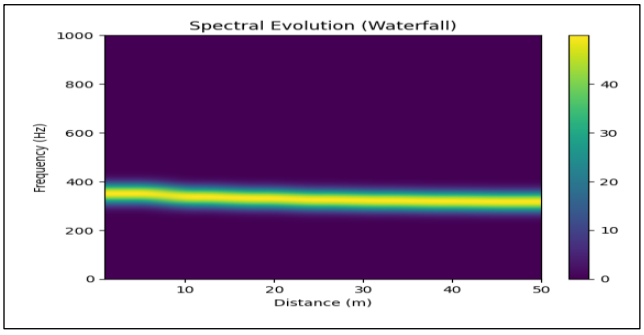

Fig. 8: Spectral Evolution (Waterfall)

The proportion of low-frequency energy increases steadily with distance, reflecting frequency-dependent attenuation mechanisms that disproportionately reduce higher-frequency content. The waterfall plot similarly indicates that the dominant spectral peak visibly shifts downward and broadens with distance, while high-

frequency energy diminishes. The plot provides a continuous visual representation of spectral evolution.

Tonal Prominence and Bandwidth Changes

The tonal prominence and bandwidth changes are as shown in table (3) and fig. (9).

Table 3: Tonal Prominence vs. Distance (ISO 1996-2)

Distance (m)	Tonal Prominence (dB)	Interpretation
1	12.5	Clearly audible
10	9.2	Audible
20	6.8	Marginal
30	4.5	Not significant
50	2.1	Not significant

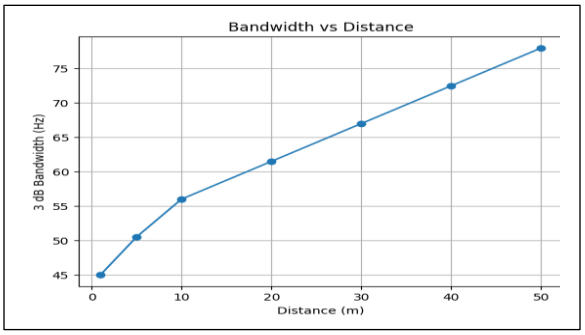

Fig. 9: 3 dB Bandwidth vs. Distance

The 3 dB bandwidth increases steadily with distance, expanding from approximately 45 Hz at 1 m to about 78 Hz at 50 m. It is observed that the tonal characteristics diminish with distance, transitioning from clearly perceptible to acoustically insignificant beyond ~30 m (Table 3). As shown in fig. (9), the spectral peak broadens with distance, indicating reduced tonal sharpness due to propagation effects and environmental scattering.

Annoyance Assessment

The annoyance assessment analysis (fig. 10) indicates that the A-weighted equivalent sound level (L_{Aeq}) decreases progressively with distance from the source. However, the low-frequency annoyance index remains positive beyond the point at which regulatory thresholds are satisfied. Notably, L_{Aeq} falls below 40 dB(A), the World Health Organization night-time guideline, at approximately 40 m. In contrast, the low-frequency annoyance index does not drop below its threshold until around 50 m, indicating a persistence of potential annoyance beyond distances deemed acceptable by conventional A-weighted criteria.

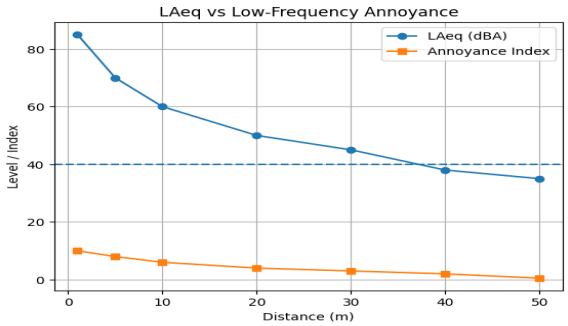

Fig. 10: L_{Aeq} and Low-Frequency Annoyance Index vs. Distance

The results shows that the A-weighted criteria indicate acceptable conditions earlier than spectral-based annoyance metrics, revealing a hidden zone of residual annoyance risk**.**

Discussion

Physical Mechanisms of Spectral Evolution

The observed downward shift in dominant frequency, from approximately 348 Hz at 1 m to about 305 Hz at 50 m, can be explained by the combined effects of frequency-dependent atmospheric absorption and ground interaction. While geometric spreading reduces sound levels uniformly across frequencies, atmospheric absorption increases strongly with frequency, leading to preferential

attenuation of higher-frequency components during propagation (ISO 9613-1:2013). As a result, the spectral balance progressively shifts toward lower frequencies with distance.

Ground effects further reinforce this trend through interference between the direct and reflected sound paths. In a simplified two-path model, phase differences between these paths produce frequency-dependent interference patterns, including spectral notches that shift with distance. For a source with a relatively broad spectral peak, attenuation on the higher-frequency side of the peak, caused by both atmospheric absorption and destructive interference, results in an apparent shift of the dominant frequency toward lower values. This mechanism is consistent with the systematic spectral migration observed in the measurements.

The increase in low-frequency proportion, from approximately 22% at source to about 41% at 50 m, follows directly from these propagation processes. Although geometric spreading affects all frequencies equally, both atmospheric absorption and ground interaction impose stronger attenuation above roughly 500 Hz. As a result, higher-frequency energy diminishes more rapidly, leaving a larger fraction of the total energy concentrated in the low-frequency range.

Comparison with Existing Studies and Standards

The magnitude of the observed dominant frequency shift exceeds predictions based solely on atmospheric absorption as described in ISO 9613-1. While the standard provides a robust framework for estimating frequency-dependent attenuation due to atmospheric conditions, it does not fully account for ground-induced interference effects. The discrepancy between predicted and observed spectral shifts therefore highlights the significant role of ground interaction and multipath propagation in shaping outdoor acoustic fields.

This finding is consistent with previous work on outdoor sound propagation, which emphasises the importance of surface impedance and reflection characteristics. However, most prior studies have focused on broadband level decay or one-third octave band analysis, rather than continuous spectral descriptors such as dominant frequency and spectral centroid. The present results extend this body of knowledge by demonstrating that these descriptors provide sensitive indicators of propagation-induced spectral changes.

From a perceptual perspective, the persistence of low-frequency dominance aligns with findings from field studies on low-frequency noise annoyance, including those by Kjell Persson Waye (Persson Waye et al., 2007; Persson Waye & Ryder, 2010). These studies show that annoyance responses are strongly influenced by low-frequency content, even when A-weighted levels are relatively low. The current results reinforce this conclusion by demonstrating that low-frequency energy becomes increasingly prominent in regions where conventional metrics suggest acceptable exposure.

The spectral mapping approach presented here therefore offers a pathway for improving exposure–response models. By incorporating physically meaningful spectral descriptors, such as low-frequency proportion and spectral centroid, it becomes possible to better represent the

acoustic factors that drive annoyance, rather than relying solely on aggregated energy-based indicators.

Implications for Low-Frequency Noise Assessment

The results indicate that regulatory approaches based solely on A-weighted sound levels at property boundaries are insufficient for sources with significant low-frequency content. A-weighting attenuates frequencies below 500 Hz by a substantial margin, leading to systematic underestimation of low-frequency energy that becomes increasingly dominant with distance. Consequently, reliance on L_{Aeq} alone may result in the misclassification of acoustically adverse environments as compliant.

A more comprehensive assessment framework should adopt a two-tier approach. The first tier would retain standard L_{Aeq}-based mapping to ensure compatibility with existing guidelines. The second tier would involve targeted spectral analysis using FFT-based methods when tonal or low-frequency characteristics are present. This approach provides a practical balance between regulatory simplicity and acoustic accuracy.

In addition, the introduction of a low-frequency penalty could improve the sensitivity of current assessment methods. For example, an adjustment of 5-10 dB could be applied when the low-frequency proportion exceeds a defined threshold (30%). Similar correction schemes already exist for tonal noise in ISO 1996-2, suggesting that such an extension is both feasible and consistent with established practice.

Overall, these findings support a shift toward frequency-aware noise assessment frameworks that explicitly account for spectral composition. Incorporating such approaches into regulatory systems would improve the alignment between measured acoustic conditions and human perception.

Methodological Reflections: Temporal Resolution and Practical Deployment

A key methodological outcome of this study is that stable spectral fingerprints can be obtained using relatively short recording durations. Specifically, time windows of 30–60 seconds were sufficient to achieve low variability in dominant frequency, spectral centroid, and low-frequency proportion. This demonstrates that reliable spectral characterisation does not require extended measurement periods, making the approach suitable for practical field applications.

This finding has important implications for environmental monitoring, as it enables the use of standard sound level meters with recording capability, as well as calibrated low-cost acoustic sensors. The ability to extract meaningful spectral information from minute-scale recordings significantly enhances the feasibility of deploying this method in routine assessments and large-scale surveys.

However, environmental measurements remain sensitive to external factors such as wind and non-stationary background noise. Wind-induced turbulence can introduce artificial low-frequency energy, potentially biasing spectral estimates. To minimise these effects, appropriate wind protection should be used, and contaminated data segments should be excluded during analysis.

Finally, the method assumes that the source is approximately stationary over the analysis period. While this assumption is valid for continuous sources such as

industrial fans, it may not hold for intermittent or time-varying sources. In such cases, shorter analysis windows or time–frequency methods, such as spectrograms, may be required to capture the full temporal dynamics of the sound field.

Conclusion

This study demonstrates that time-domain acoustic measurements combined with FFT-based spectral analysis provide a robust framework for characterising the spatial evolution of environmental noise. Unlike conventional A-weighted metrics, which suggest monotonic attenuation with distance, the results reveal a systematic redistribution of spectral energy toward lower frequencies, accompanied by a measurable downward shift in dominant frequency and increasing low-frequency proportion with propagation distance.

The findings show that atmospheric absorption and ground-induced interference jointly reshape the spectral signature of stationary sources in ways that are not captured by standard $_{LAeq}$-based assessment methods. Notably, low-frequency energy becomes increasingly dominant at greater distances, resulting in sustained annoyance potential even where regulatory A-weighted thresholds are satisfied. A minimum 30-second recording window was also identified as sufficient for stable spectral extraction, supporting practical field deployment of the method.

Overall, the study provides strong evidence for integrating frequency-aware descriptors into environmental noise assessment frameworks. Incorporating FFT-derived spectral metrics alongside conventional indicators would improve the physical and perceptual accuracy of noise mapping, particularly for low-frequency-dominated sources in complex outdoor environments.

References

Attenborough, K., Li, K. M., & Horoshenkov, K. V. (2014). Predicting outdoor sound propagation. *Applied Acoustics, 76*, 1–3.

Basner, M., Babisch, W., Davis, A., et al. (2014). Auditory and non-auditory effects of noise on health. *The Lancet, 383*(9925), 1325–1332.

Berglund, B., Lindvall, T., & Schwela, D. H. (2013). *Guidelines for Community Noise*. WHO update discussions and extensions.

Brigham, E. O. (1988). *The Fast Fourier Transform and Its Applications*. Englewood Cliffs, NJ: Prentice Hall.

Castellengo, M. (2010). Low-frequency noise and vibroacoustic effects. *Acoustics Research Letters Online*.

European Parliament & Council (2002). Directive 2002/49/EC relating to the assessment and management of environmental noise.

Fastl, H., & Zwicker, E. (2007). *Psychoacoustics: Facts and Models*. Springer.

Hayes, M. H. (2013). *Statistical Digital Signal Processing and Modeling*. Wiley.

IEC (2009). IEC 61672-1: Electroacoustics-Sound level meters.

ISO 9613-1:2013. Attenuation of sound during propagation outdoors.

ISO (2017). ISO 1996-2: Description, measurement and assessment of environmental noise.

Leventhall, H. G. (2010). Low frequency noise: What we know, what we do not know. *Journal of Low Frequency Noise, Vibration and Active Control, 29*(2), 97–144.

Münzel, T., Sørensen, M., Gori, T., Schmidt, F. P., Rao, X., Brook, J., Chen, L. C., Brook, R. D., & Rajagopalan, S. (2021). Environmental noise and the cardiovascular system. *European Heart Journal, 42*(26), 2387–2401.

Oppenheim, A. V., & Schafer, R. W. (2010). *Discrete-time signal processing* (3rd ed.). Pearson.

Pawlaczyk-Łuszczyńska, M., Dudarewicz, A., Zaborowski, K., & Zamojska-Daniszewska, A. (2014). Annoyance from low-frequency noise. *International Journal of Occupational Medicine and Environmental Health, 27*(5), 774–789.

Persson Waye, K., Bengtsson, J., Rylander, R., & Hucklebridge, F. (2007). *Low frequency noise "pollution" interferes with performance*. Noise and Health, 9(37), 33–39.

Persson Waye, K., & Rylander, R. (2010). The prevalence of annoyance and effects of low-frequency noise. *Journal of Sound and Vibration, 330*(1), 112–119.

Penney, R., et al. (2014). Psychoacoustic metrics and environmental noise perception. *Applied Acoustics, 84*, 1-10.

Ryherd, E. E., & Okcu, S. (2014). Psychoacoustic considerations in environmental noise assessment. *Applied Acoustics, 83*, 1-10.

Stoica, P., & Moses, R. L. (2013). *Spectral analysis of signals*. Pearson.

WHO (2018). *Environmental Noise Guidelines for the European Region*. World Health Organization.

Zwicker, E., & Fastl, H. (2013). *Psychoacoustics: Facts and Models* (3rd ed.). Springer.